2023

Electromagnetic Radiation from a Spherical Static Current Source Coupled to Harmonic Axion Field

Railing Chang
National Taiwan Ocean University

Huai-Yi Xie
Institute of Nuclear Energy Research

P. T. Leung
Portland State University, hopl@pdx.edu

Citation Details

Chang, R., Xie, H. Y., & Leung, P. T. (2023). [PRE-PRINT] Electromagnetic radiation from a spherical static current source coupled to harmonic axion field. Physics Letters A, 128991.

Electromagnetic radiation from a spherical static current source coupled to harmonic axion field

Railing Chang[1*], Huai-Yi Xie[2], and P. T. Leung[3]

[1] *Department of Optoelectronics and Materials Technology, National Taiwan Ocean University, Keelung, Taiwan*
[2] *Division of Physics, Institute of Nuclear Energy Research, Taoyuan County 32546, Taiwan*
[3] *Department of Physics, Portland State University, P. O. Box 751, Portland, Oregon 97207, USA*

Abstract

The electromagnetic fields generated from a static current source on a spherical surface are calculated in the framework of axion electrodynamics to first order in the coupling parameter. Comparisons of the results are made with reference to various results obtained in conventional Maxwell electrodynamics, as well as previous results obtained for point magnetic dipole source coupled to harmonic axion fields. Distinct features from the results so obtained are highlighted for possible experimental probing of the axions via electromagnetic interactions. In particular, electromagnetic radiation from sources with strong magnetic field is studied which may enable the detection of a cosmic axion field from its interaction with objects like neutron stars.

KEY WORDS: particle dark matter; axion electrodynamics

* Corresponding author: rlchang@ntou.edu.tw

Introduction

Since its first conception in the late 1970's for the resolution of the "strong CP problem" [1-3], the axion has become one of the most elusive particles which has received intensive studies among researchers for its possible relevance to the understanding of the dark matter cosmos (for more recent references, see, e.g. [4-6]). Upon recognizing the possibility of axion-photon interactions, Sikivie was the first to formulate axion electrodynamics (AED) and to propose electromagnetic (EM) setups for the detection of this elusive particle [7]. This was followed by Wilczek in his application of AED to account for the dyon fractional charge, and to extend its relevance to condensed matter physics via the quantized Hall effect [8]. It is of interest for AED to be indeed finally realized in condensed matter systems with the discovery of topological insulators in the late 2000's [9-11].

While the search for axionic dark matter via electromagnetic interaction is still an ongoing effort with tremendous activities in recent years [4-6], device with strong magnetic fields (both static and oscillating) are still most often applied in experimental studies [6]. Hence the understanding of how EM fields behave with various current sources in a cosmic axion background will be of significance for these experimental search of axions. Most often, current source of cylindrical geometry such as that with an infinite solenoid is considered which can have experimental relevance, as well as for its relative simplicity in the mathematical solutions [12]. Moreover, a cylindrical solenoid of finite length in AED will be a very challenging mathematical problem to be solved.

It is the purpose of our present work to study the EM fields from a static current source on a spherical surface coupled to an oscillating cosmic axion field background (Fig. 1). This can be a constantly-rotating spherical shell with a uniform surface charge for which the magnetostatic solutions in conventional (Maxwell) EM theory are well-known, that is: a uniform magnetic field inside the shell and an exactly dipolar field outside the sphere [13]. The results obtained will be useful for the possible detection of the axion via its interaction with stellar objects which possess strong magnetic fields. In the following we will provide the exact solution for this problem in AED and shall compare the results with those well-known results from Maxwell's EM theory, as well as from previously-published results for point magnetic dipoles in AED [14]. Distinct features will be highlighted with anticipation that the results will provide alternative EM probes of the axion in future experiments.

Theory

Consider the following classic example in magnetostatics with a uniform total charge $Q_T = 4\pi a^2 \sigma$ distributed on a spherical surface of radius a, rotating in vacuum with a constant angular velocity ω_0 about the z axis, thus producing a constant surface current density $\boldsymbol{J} = \sigma\omega_0 a \sin(\theta)\delta(r-a)\mathbf{e}_{\vartheta} \equiv J_0 \sin(\theta)\delta(r-a)\mathbf{e}_{\vartheta}$. In the conventional Maxwell's theory, the solution is well-known to be an exact magnetic dipole field outside the sphere with a dipole moment $\boldsymbol{m} = \frac{Q_T \omega_0 a^2}{3c}\boldsymbol{e}_z = \frac{V}{c} J_0 \boldsymbol{e}_z$ with V the volume of the sphere; while inside the sphere the field is uniform given by $\boldsymbol{B}_{in} = \frac{2}{a^3}\boldsymbol{m}$ [13]. Our problem here is to re-calculate the electromagnetic (EM) fields both inside and outside the sphere in the presence of a harmonic cosmic axion field of the form $\Theta = \theta_0 e^{-i\omega t}$. The results will be applicable to a source with uninform magnetic field (in the absence of the axion) in a spherical region, whatever that origin is for the magnetic field. In axion electrodynamics, the field equations are well-known to have the following modified form (in Gaussian units) [7, 12, 14]:

$$\begin{aligned}
&\nabla\cdot\boldsymbol{E} = 4\pi\rho - 4\pi g_a \nabla\Theta\cdot\boldsymbol{B}\\
&\nabla\cdot\boldsymbol{B} = 0\\
&\nabla\times\boldsymbol{E} + \frac{1}{c}\frac{\partial\boldsymbol{B}}{\partial t} = 0\\
&\nabla\times\boldsymbol{B} - \frac{1}{c}\frac{\partial\boldsymbol{E}}{\partial t} = \frac{4\pi}{c}\boldsymbol{J} + 4\pi g_a\left[\frac{1}{c}\frac{\partial\Theta}{\partial t}\boldsymbol{B} + \nabla\Theta\times\boldsymbol{E}\right]
\end{aligned}, \tag{1}$$

where g_a is the axion-photon coupling constant. Note that the equations in (1) are derived from a Lagrangian density of the form $\mathsf{L} = -\frac{1}{16\pi}F_{\beta\gamma}F^{\beta\gamma} - \frac{1}{c}J_\beta A^\beta - \frac{1}{8}g_\alpha\Theta\varepsilon^{\beta\gamma\delta\rho}F_{\beta\gamma}F_{\delta\rho}$ where the dynamics of the axion field is not explicitly included, since here we have assumed a cosmic background of harmonic axion field (of given amplitude and frequency) as was considered in the previous studies [12, 14]. Following these previous works [12, 14], we start by ignoring the spatial gradient term of the axion field in Eq. (1) due to the de Broglie wavelength of the axion being much greater than the oscillation wavelength as well as the size of the sphere. In addition, we shall also assume a weak axion-photon coupling and calculate the EM fields to first order in the coupling constant as was done in the previous works [12, 14]. Hence we let:

$$\boldsymbol{E}(\boldsymbol{r},t) = \boldsymbol{E}_0(\boldsymbol{r},t) + \boldsymbol{E}_1(\boldsymbol{r},t) + O\left(g_a^{\ 2}\right), \tag{2}$$

$$\boldsymbol{B}(\boldsymbol{r},t) = \boldsymbol{B}_0(\boldsymbol{r},t) + \boldsymbol{B}_1(\boldsymbol{r},t) + O\left(g_a^{\ 2}\right). \tag{3}$$

With all these into Eq. (1), and assuming all field quantities to have the same time dependence of the axion field, we finally obtain the following systems of field equations for each of the unperturbed and first order fields as follows:

$$\begin{aligned}
&\nabla \cdot \boldsymbol{E}_0 = 0 \\
&\nabla \cdot \boldsymbol{B}_0 = 0 \\
&\nabla \times \boldsymbol{E}_0 = 0 \\
&\nabla \times \boldsymbol{B}_0 = \frac{4\pi}{c}\boldsymbol{J}
\end{aligned} \quad , \tag{4}$$

and

$$\begin{aligned}
&\nabla \cdot \boldsymbol{E}_1 = 0 \\
&\nabla \cdot \boldsymbol{B}_1 = 0 \\
&\nabla \times \boldsymbol{E}_1 - ik\boldsymbol{B}_1 = 0 \\
&\nabla \times \boldsymbol{B}_1 + ik\boldsymbol{E}_1 = -4\pi i g_a k \Theta \boldsymbol{B}_0
\end{aligned} \quad , \tag{5}$$

where $k = \frac{\omega}{c}$. With $\boldsymbol{J}$ in (4) the constant spherical surface current described above, the unperturbed magnetic field is simply given by the well-known solution:

$$\boldsymbol{B}_0 = \begin{cases} \dfrac{3(\boldsymbol{m} \cdot \boldsymbol{e}_r)\boldsymbol{e}_r - \boldsymbol{m}}{r^3} \ , \ a < r \\ \dfrac{2}{a^3}\boldsymbol{m} \ , \qquad r < a \end{cases} , \tag{6}$$

with $\boldsymbol{m}$ the magnetic dipole moment defined above. To calculate the first order fields, we first obtain the Helmholtz equations from (5) as follows:

$$\nabla^2 \boldsymbol{E}_1 + k^2 \boldsymbol{E}_1 = -4\pi g_a k^2 \theta_0 \boldsymbol{B}_0 \quad , \tag{7}$$

$$\nabla^2 \boldsymbol{B}_1 + k^2 \boldsymbol{B}_1 = 4\pi i g_a k \theta_0 \nabla \times \boldsymbol{B}_0 = \frac{(4\pi)^2}{c} i g_a k \theta_0 \boldsymbol{J} \quad , \tag{8}$$

where we have used Eq. (4) in the last step of Eq. (8), and all field quantities are the spatial parts with the harmonic time factor suppressed. Next, we are going to calculate the first order fields by expanding them into vector spherical multipoles. Following Jackson [13], Eq. (7) leads to:

$$\nabla^2 (\boldsymbol{r} \cdot \boldsymbol{E}_1) + k^2 (\boldsymbol{r} \cdot \boldsymbol{E}_1) = -4\pi g_a k^2 \theta_0 (\boldsymbol{r} \cdot \boldsymbol{B}_0). \tag{9}$$

Using Eq. (8) and with the help of the Heaviside step function, we obtain:

$$\boldsymbol{r}\cdot\boldsymbol{B}_0=\sqrt{\frac{16\pi}{3}}mSY_{10} \quad , \tag{10}$$

where $m=|\boldsymbol{m}|$, $Y_{10}=\sqrt{3/4\pi}\cos\theta$ is the spherical harmonic, and

$$S\equiv\frac{1}{r^2}\vartheta(r-a)+\frac{r}{a^3}\vartheta(a-r), \tag{11}$$

with ϑ being the Heaviside step function. With the application of the Green's function (Eq. (A8) in the Appendix) and by expanding it in terms of the multipole spherical waves [13], Eq. (9) with the source term given in Eq. (10) can finally be integrated to yield:

$$\boldsymbol{r}\cdot\boldsymbol{E}_1(\boldsymbol{r})=\sqrt{\frac{16\pi}{3}}ikmf_1(kr)Y_{10}(\theta,\varphi)\left(4\pi g_a k^2\theta_0\right), \tag{12}$$

with the radial function obtained in terms of the various spherical Bessel functions as follows:

For $r>a$,

$$f_1(kr)=\frac{1}{k}h_0^{(1)}(kr)j_1(kr)-\left[\frac{j_0(kr)}{k}-\frac{3}{k^2a}j_1(ka)\right]h_1^{(1)}(kr), \tag{13}$$

For $r<a$,

$$\begin{aligned}f_1(kr)=&\left[\frac{r^3}{ka^3}h_0^{(1)}(kr)-\frac{3r^2}{k^2a^3}h_1^{(1)}(kr)+\frac{3}{k^2a}h_1^{(1)}(ka)\right]j_1(kr)\\&-\left[\frac{r^3}{ka^3}j_0(kr)-\frac{3r^2}{k^2a^3}j_1(kr)\right]h_1^{(1)}(kr)\end{aligned}\quad. \tag{14}$$

To extract $\boldsymbol{E}_1$ from (12), we go back to the fourth equation in (5) and obtain

$$\boldsymbol{r}\cdot\boldsymbol{E}_1=-\frac{1}{k}\boldsymbol{L}\cdot\boldsymbol{B}_1-4\pi g_a\theta_0\boldsymbol{r}\cdot\boldsymbol{B}_0, \tag{15}$$

where the operator $\boldsymbol{L}\equiv\frac{1}{i}\boldsymbol{r}\times\nabla$. From (10), (12) and (15), we can calculate $\boldsymbol{L}\cdot\boldsymbol{B}_1$ and obtain:

$$\boldsymbol{L}\cdot\boldsymbol{B}_1=-16\sqrt{\frac{\pi^3}{3}}g_a\theta_0 m\left\{ik^4 f_1(kr)+kS\right\}Y_{10}(\theta,\varphi), \tag{16}$$

where the function S is defined as in Eq. (11). Eq. (16) yields directly the following results for the first order fields:

$$\boldsymbol{B}_1=-16\sqrt{\frac{\pi^3}{3}}g_a\theta_0 m\left\{ik^4 f_1(kr)+kS\right\}\frac{\boldsymbol{L}Y_{10}(\theta,\varphi)}{2}\ , \tag{17}$$

$$\boldsymbol{E}_1=\frac{1}{-ik}\left(\nabla\times\boldsymbol{B}_1+4\pi g_a k\theta_0\boldsymbol{B}_0\right)\ , \tag{18}$$

where the electric field is obtained from Ampere’s law in (6). Using Eqs. (6) and (17), and the following result:

$$m\boldsymbol{L}Y_{10}(\theta,\varphi)=\sqrt{\frac{3}{4\pi}}\left(i\frac{\boldsymbol{m}\times\boldsymbol{r}}{r}\right), \tag{19}$$

Eq. (18) finally leads to the following result for the electric field:

$$\boldsymbol{E}_1=4\pi i g_a\theta_0 k^3\left[rP_r\boldsymbol{m}+2P\boldsymbol{m}-P_r\left(\boldsymbol{m}\cdot\boldsymbol{e}_r\right)\boldsymbol{r}\right]\ , \tag{20}$$

where $P\equiv\frac{f_1(kr)}{r}$ and $P_r\equiv\frac{\partial P}{\partial r}$. Furthermore, the magnetic field can also be obtained from Eqs. (17) and (19) as follows:

$$\boldsymbol{B}_1=-4\pi i g_a\theta_0\left[ik^4 f_1(kr)+kS\right]\frac{\boldsymbol{m}\times\boldsymbol{r}}{r}. \tag{21}$$

Point magnetic dipole fields

As a check of our results for the spherical surface current source, we look at the limit when the sphere radius goes to zero and compare with the results for a point magnetic dipole source as published previously in the literature [14].

To do this, we look at the limit of the result in Eq. (13) as $a \to 0$. Using the explicit form of the spherical Bessel and Hankel functions, together with the following result for small ka:

$$j_1(ka) \approx \frac{1}{3} ka \, , \tag{22}$$

Eq. (13) reduces to the following as $a \to 0$:

$$f_1(kr) \approx \frac{i}{k^3 r^2} - \frac{e^{ikr}}{k^2 r}\left(1 + \frac{i}{kr}\right) \, . \tag{23}$$

Using this, one can calculate the quantity in the bracket in Eq. (20) to obtain:

$$rP_r \boldsymbol{m} + 2P\boldsymbol{m} - P_r(\boldsymbol{m}\cdot\boldsymbol{e}_r)\boldsymbol{r} \approx \frac{e^{ikr}}{ik^3}\left[\left(e^{-ikr} + ikr - 1\right)\frac{1}{r^3}\left(\boldsymbol{m} - 3(\boldsymbol{m}\cdot\boldsymbol{e}_r)\boldsymbol{e}_r\right) + k^2\frac{1}{r}\left(\boldsymbol{m} - (\boldsymbol{m}\cdot\boldsymbol{e}_r)\boldsymbol{e}_r\right)\right]. \tag{24}$$

With this into Eq. (20), we obtain:

$$\boldsymbol{E}_1 \approx 4\pi g_a \theta_0 e^{ikr}\left[\left(e^{-ikr} + ikr - 1\right)\frac{1}{r^3}\left(\boldsymbol{m} - 3(\boldsymbol{m}\cdot\boldsymbol{e}_r)\boldsymbol{e}_r\right) + k^2\frac{1}{r}\left(\boldsymbol{m} - (\boldsymbol{m}\cdot\boldsymbol{e}_r)\boldsymbol{e}_r\right)\right]. \tag{25}$$

The result in (25) is consistent with the electric field due to a static magnetic point dipole coupled to a harmonic time-dependent axion field as worked out previously in the literature [14, see Appendix]. Similarly, we can obtain the corresponding magnetic field in the point dipole limit from Eq. (21) by substituting (11) (for $r > a$) and (23) into (21). We thus obtain:

$$\boldsymbol{B}_1 \approx -4\pi i g_a \theta_0\left[ik\frac{i}{r^2} - ik^2\frac{e^{ikr}}{r}\left(1 + \frac{i}{kr}\right) + \frac{k}{r^2}\right]\frac{\boldsymbol{m}\times\boldsymbol{r}}{r},$$

which simplifies to the following, again consistent with that in [14]:

$$\boldsymbol{B}_1 \approx -4\pi i g_a k\theta_0 e^{ikr}\left(\frac{1}{r^3} - \frac{ik}{r^2}\right)\boldsymbol{m}\times\boldsymbol{r} \, . \tag{26}$$

Radiation from static spherical current source

One of the most interesting consequences of coupling to a harmonic axion field is the possibility of EM radiations from a *static* distribution of current [6, 14]. In this section, we shall calculate the far fields emitted by the static current on a finite sphere of unlimited size, and the radiation intensity from its coupling to the axion field. Thus in the far zone, only the spherical Hankel function survives in Eq. (13) and to $O\left(\frac{1}{r}\right)$ we have:

$$f_1(kr) \approx Q(a)\frac{e^{ikr}}{kr} \ , \tag{27}$$

where the "finite size factor" is defined as:

$$Q(a) \equiv -\frac{3}{k^2 a} j_1(ka) . \tag{28}$$

Using this for the calculation of $P \equiv \frac{f_1(kr)}{r}$ and $P_r \equiv \frac{\partial P}{\partial r}$ in Eq. (20), we finally obtain to $O\left(\frac{1}{r}\right)$ the following far field result for the electric field:

$$\boldsymbol{E}_1 \to -4\pi g_a \theta_0 k^3 e^{ikr}\left[\frac{\boldsymbol{m}}{r} - \frac{(\boldsymbol{m}\cdot\boldsymbol{r})\boldsymbol{r}}{r^3}\right] Q(a) . \tag{29}$$

Similarly, using (11) (for $r > a$) and (27) into (21), we obtain to $O\left(\frac{1}{r}\right)$:

$$\boldsymbol{B}_1 \to 4\pi g_a \theta_0 k^3 e^{ikr}\frac{\boldsymbol{m}\times\boldsymbol{r}}{r^2} Q(a) . \tag{30}$$

Note that as $a \to 0$ and $Q(a) \to -\frac{1}{k}$, both results in (29) and (30) agree with the far fields due to a point magnetic dipole. We next calculate the radiated power from the fields in (29) and (30).

Since the static source current corresponding to the field $\boldsymbol{B}_0$ does not radiate, the total radiation when coupled to the harmonic axion field will be determined exclusively by the fields in (29) and (30). Thus we have the time-averaged Poynting vector given by:

$$\langle \boldsymbol{S} \rangle = \frac{c}{8\pi} \mathrm{Re}\left(\boldsymbol{E}_1 \times \boldsymbol{B}_1 \right) = 2\pi c \left[g_a \theta_0 k^3 \frac{m}{r} Q(a) \right]^2 \sin^2\theta \, \boldsymbol{e}_r , \qquad (31)$$

along the radial direction from the center of the sphere with θ the angle between the observer and the direction of the magnetic dipole moment. From this, we obtain the differential radiated power to be:

$$\frac{dP}{d\Omega} = 2\pi g_a^2 \theta_0^2 m^2 c k^6 Q(a)^2 \sin^2\theta , \qquad (32)$$

which reduces to the result for a point magnetic dipole as $a \to 0$ [14]:

$$\left(\frac{dP}{d\Omega} \right)_0 = 2\pi g_a^2 \theta_0^2 m^2 c k^4 \sin^2\theta . \qquad (33)$$

It is interesting that the finite sphere case turns out to radiate with an angular dependence just like a point dipole case, despite the field solutions are quite distinct between the two in the presence of the axion. Moreover, Eq. (32) a result for the differential radiation power from a spherical source of unlimited size as indicated by the size factor $Q(a)$. As a consequence, significant deviation in the radiation intensity from that of a point dipole source can occur for a large sphere as illustrated by the following numerical analysis.

Numerical Results

In this section we shall present some numerical results with the wave number given by the axion Compton wavelength via $k = 2\pi/\lambda_a$. We first look at some sample field amplitudes both inside and outside the sphere. Figure 2 shows a plot of the real and imaginary parts of the axion-induced electric and magnetic fields as a function of position (normalized to λ_a) at

$\theta = 90^0$ for two sizes of the sphere. We see that while all the field components oscillate and decay as the observer goes farther away from the sphere, the larger sphere will have these induced fields oscillate more rapidly. This is similar to the case with an infinite cylinder geometry [12]. Moreover, this is in sharp contrast with the case in the absence of the axion field where the field inside the sphere is an exactly uniform magnetic field. Hence detection of small oscillatory nonuniformity in the inside magnetic field can provide evidence for the presence of the axion field, when one has a uniform static current source of axial symmetry on a spherical shell. In addition, we have also observed (not shown) non-oscillating behavior for the fields as well as the suppression of the induced electric field [12] for smaller spheres $\left(e.g.,\ a = 0.01\lambda_a\right)$.

Next we compare with the axion-induced fields for a spherical current of finite radius with those from a point magnetic dipole moment [14]. Figure 3 shows again the different field components for two different sphere sizes in comparison with the case of a point magnetic dipole source, for a fixed dipole moment. It is seen that the finite sphere results are quite different and are smaller than those for the point magnetic dipole source, again a result in sharp contrast with the fields in the pure Maxwellian case in which the field outside the sphere is expected to be identical to those of a point magnetic dipole.

Finally, we study the radiation power due to these axion-induced fields. First it is interesting to note that the angular distributions from Eqs. (32) and (33) are the same and are of typical "dipole radiation characteristics" ($\sim \sin^2\theta$), despite the finite size of the sphere. Figure 4 shows a few plots for different sphere sizes and it is seen that for a fixed dipole moment, the radiation can be several orders of magnitude weaker as the size is increased for the sphere. In fact, this radiation is expected to be extremely weak due to the small values of the axion-photon coupling and the axion field amplitude [6, 14]. However, for astrophysical objects with highly intense magnetic fields like the neutron star [6], the maximum power radiated in the $\theta = 90^0$ direction can be estimated from Eq. (32) to be of a magnitude

$$\sim 2\pi\left(10^{-21}\right)^2\left(\tfrac{1}{2}B_0a^3\right)^2 c\left(\tfrac{2\pi}{\lambda_a}\right)^6 Q(a)^2 \text{ erg/s} \quad , \qquad (34)$$

where we have adopted a value of $g_a\theta_0 \sim 10^{-21}$ [14], and with a value of magnetic field $B_0 \sim 10^{13} G$ [6] and a radius $a \sim 2km$ for the neutron star, (34) yields of a power of ~ 0.042 watt if we assume a value of axion wavelength $\lambda_a \sim 60\ cm$ [12]. Such small value of radiation power for radio / microwaves may not be unmeasurable (e.g. from space lab.) with current technology.

Conclusion

In this work, we have provided analytical solutions for the electromagnetic fields from a spherical static current interacting with a harmonic axion field, calculated to first order of the axion-photon coupling constant. This is complementary to the previous work which has considered a current with cylindrical symmetry [12]. From the results we obtained, we have highlighted several distinct features as follows. These include the oscillatory nonuniformity of the magnetic field inside the sphere, as well as the possibly measurable long wavelength EM radiation from the axion-magnetic field interaction with a neutron star. In addition, we have also studied the difference between our present results and those from previous literature for the fields from a point magnetic dipole interacting with the axion [14]. In doing so, we have clarified that the contact fields from a point magnetic dipole are not affected by the presence of the axion [see Appendix]. We believe these results will be useful for future electromagnetic probes of the cosmological axion.

Appendix

Here we re-derive the electromagnetic fields due to a static current of a point magnetic dipole in coupling with a harmonic time-dependent axion field using the Green dyadic approach. In the literature, these were first obtained by Hill in his demonstration of the induced electric dipole moment for the electron coupled to such an axion field [14]. Moreover, a sourceless magnetic field had been considered and the possible effects on the contact terms were not studied. Here we show explicitly that the contact term will not be affected by the coupling with the axion field.

By recalling the vector wave equations in Eqs. (7) and (8) for the first order EM fields:

$$\nabla^2 \boldsymbol{E}_1 + k^2 \boldsymbol{E}_1 = -4\pi g_a k^2 \theta_0 \boldsymbol{B}_0 \quad , \tag{A1}$$

$$\nabla^2 \boldsymbol{B}_1 + k^2 \boldsymbol{B}_1 = 4\pi i g_a k \theta_0 \nabla \times \boldsymbol{B}_0 \, , \tag{A2}$$

we see that these are completely analogous to the Maxwell vector wave equations with the source current being replaced by the ordinary point magnetic dipole field with the source term [13]:

$$\boldsymbol{B}_0(\boldsymbol{r}) = \frac{8\pi}{3} \boldsymbol{m} \delta(\boldsymbol{r}) + \frac{3(\boldsymbol{m} \cdot \boldsymbol{e}_r)\boldsymbol{e}_r - \boldsymbol{m}}{r^3} \quad . \tag{A3}$$

Hence the first order EM fields can be solved with the application of the well-known electric and magnetic dyadic Green functions [15] to obtain:

$$\boldsymbol{E}_1(\boldsymbol{r}) = 4\pi\kappa k^2 \theta_0 \int \boldsymbol{G}_e(\boldsymbol{r},\boldsymbol{r}') \cdot \boldsymbol{B}_0(\boldsymbol{r}') d^3x' \, , \tag{A4}$$

$$\boldsymbol{B}_1(\boldsymbol{r}) = -4\pi i \kappa k \theta_0 \int \boldsymbol{G}_m(\boldsymbol{r},\boldsymbol{r}') \cdot \boldsymbol{B}_0(\boldsymbol{r}') d^3x' , \tag{A5}$$

where the dyadic Green functions can be obtained from the scalar Green function as follows:

$$\boldsymbol{G}_e(\boldsymbol{r},\boldsymbol{r}') = \left(\boldsymbol{I} + \frac{1}{k^2} \nabla \cdot \nabla \right) G_0(\boldsymbol{r},\boldsymbol{r}') \quad , \tag{A6}$$

$$\boldsymbol{G}_m\left(\boldsymbol{r},\boldsymbol{r}'\right)=\nabla\times\boldsymbol{I}G_0\left(\boldsymbol{r},\boldsymbol{r}'\right), \tag{A7}$$

with

$$G_0\left(\boldsymbol{r},\boldsymbol{r}'\right)=\frac{e^{ik\left|\boldsymbol{r}-\boldsymbol{r}'\right|}}{4\pi\left|\boldsymbol{r}-\boldsymbol{r}'\right|} \quad . \tag{A8}$$

With (A3), (A6), and (A8) into (A4), and using the following singular double derivatives for the Coulomb function established in the literature [16]:

$$\partial_p\partial_q\left(\frac{1}{r}\right)=-\frac{4\pi}{3}\delta_{pq}\delta\left(\boldsymbol{r}\right)+\frac{3x_px_q-r^2\delta_{pq}}{r^5}, \tag{A9}$$

it can be shown, after some algebra, the first order electric field from a static point magnetic dipole coupled to a harmonic axion field to be given by the following expressi

$$\boldsymbol{E}_1\left(\boldsymbol{r}\right)=4\pi g_a\theta_0 e^{ikr}\left[\frac{1}{r^3}\left(\boldsymbol{m}-3\left(\boldsymbol{m}\cdot\boldsymbol{e}_r\right)\boldsymbol{e}_r\right)\left(e^{-ikr}+ikr-1\right)+\frac{k^2}{r}\left(\boldsymbol{m}-\left(\boldsymbol{m}\cdot\boldsymbol{e}_r\right)\boldsymbol{e}_r\right)\right]. \tag{A10}$$

Similarly, substituting (A3), (A7), (A8) into (A5) and using (A9), one obtains the corresponding first order magnetic field as follows:

$$\boldsymbol{B}_1\left(\boldsymbol{r}\right)=-4\pi i g_a k\theta_0 e^{ikr}\boldsymbol{m}\times\boldsymbol{r}\left(\frac{1}{r^3}-\frac{ik}{r^2}\right). \tag{A11}$$

Note that the results in (A10) and (A11) are consistent with those obtained by Hill for a sourceless magnetic dipole field, except our signs here are different than those in [14]. These results agree exactly with those in Eqs. (25) and (26). Moreover, in our present derivation which incorporates the contact term in (A3), we have demonstrated explicitly that the source (contact) term is not affected by the coupling of the magnetic dipole with the axion field, and the results can check consistently with those from the "infinitesimal small limit" of the results obtained for a finite sphere of uniform static current source as we have demonstrated.

References

[1] R. D. Peccei and H. R. Quinn, Phys. Rev. Lett. **38**, 1440 (1977).

[2] S. Weinberg, Phys. Rev. Lett. **40**, 223 (1978).

[3] F. Wilczek, Phys. Rev. Lett. **40**, 279 (1978).

[4] N. Blinov, M. J. Dolan, P. Draper, and J. Kozaczuk, Phys. Rev. D **100**, 015049 (2019).

[5] J. A. Dror, H. Murayama, and N. L. Rodd, Phys. Rev. D **103**, 115004 (2021).

[6] P. Sikivie, Rev. Mod. Phys. **93**, 015004 (2021).

[7] P. Sikivie, Phys. Rev. Lett. **51**, 1415 (1983).

[8] F. Wilczek, Phys. Rev. Lett. **58**, 1799 (1987).

[9] X.-L. Qi, T. L. Hughes and S.-C. Zhang, Phys. Rev. B **78**, 195424 (2008).

[10] M. Z. Hasan and C. L. Kane, Rev. Mod. Phys. **82**, 3045 (2010).

[11] X.-L. Qi and S.-C. Zhang, Rev. Mod. Phys. **83**, 1057 (2011).

[12] J. Ouellet and Z. Bogorad, Phys. Rev. D **99**, 055010 (2019).

[13] J. D. Jackson, Classical Electrodynamics (Wiley, New York, 1998).

[14] C. T. Hill, Phys. Rev. D **93**, 025007 (2016).

[15] C.-T. Tai, Dyadic Green Function in Electromagnetic Theory (IEEE, New York, 1994).

[16] C. P. Frahm, Am. J. Phys. **51**, 826 (1983).

Figure Captions

1. Geometry of the problem with a harmonic axion field $\Theta = \theta_0 e^{-i\omega t}$.

2. Electromagnetic field strengths in unit of ($4\pi g\theta_0 B_0$) as a function of observer distance from the center of the sphere for two sizes of the sphere.

3. Comparison of the field strengths from a spherical current with those from a point magnetic dipole source, again for two sphere sizes. The fields are in unit of ($\frac{4\pi g\theta_0 m}{\lambda_a^3}$).

4. Angular distribution of radiation power for two different sphere sizes, in comparison with that from a magnetic point dipole source. The power is plotted in unit of $c\left(\frac{g\theta_0 m}{\lambda_a^2}\right)^2$.

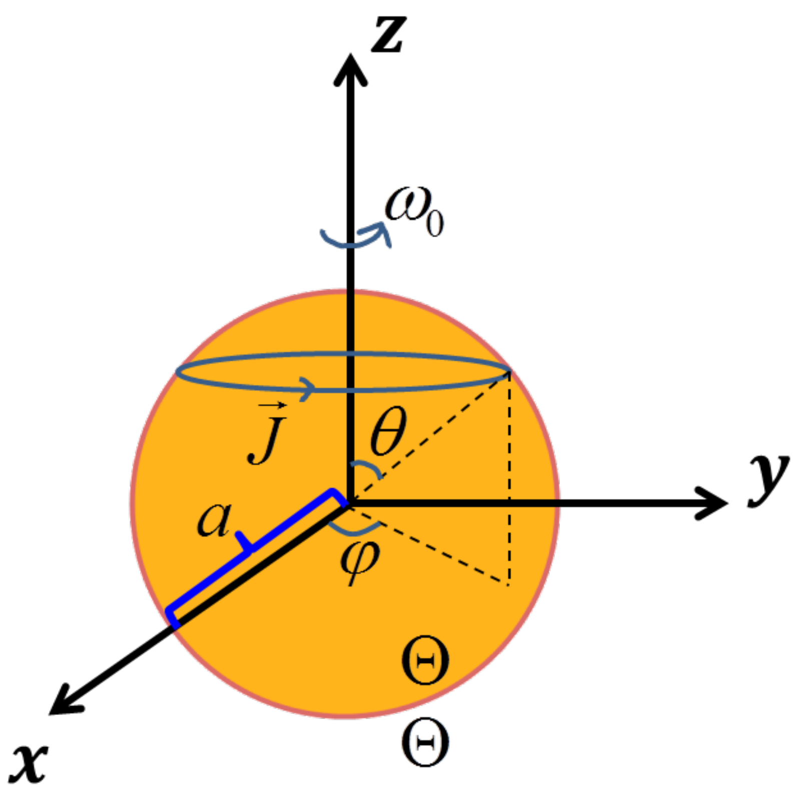

Fig. 1

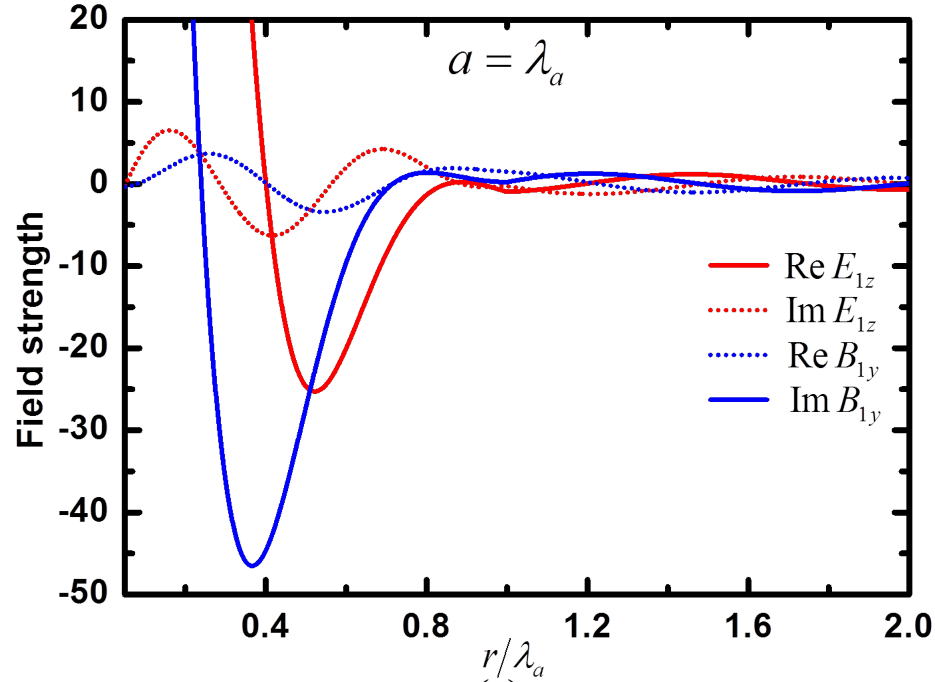
$a = \lambda_a$
Re E_{1z}
Im E_{1z}
Re B_{1y}
Im B_{1y}
Field strength
r/λ_a
20
10
0
-10
-20
-30
-40
-50
0.4
0.8
1.2
1.6
2.0

(a)

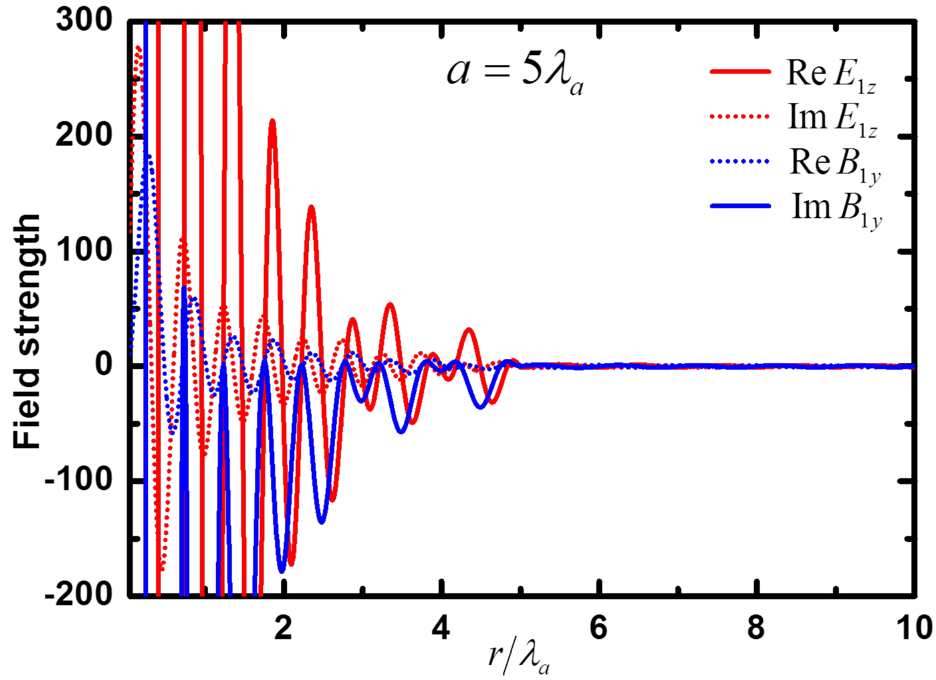
$a = 5\lambda_a$
Re E_{1z}
Im E_{1z}
Re B_{1y}
Im B_{1y}
Field strength
r/λ_a
300
200
100
0
-100
-200
2
4
6
8
10

(b)

Fig. 2

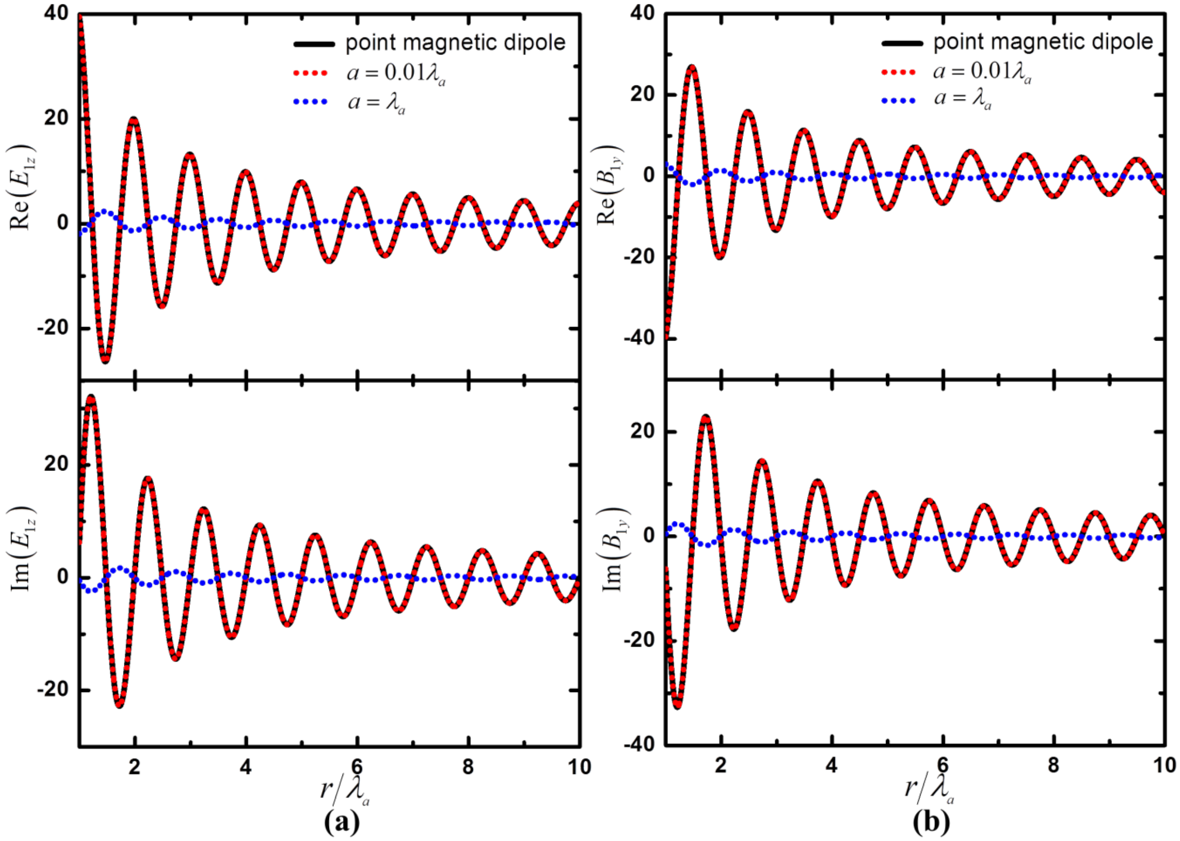

point magnetic dipole
$a = 0.01\lambda_a$
$a = \lambda_a$
$\mathrm{Re}(E_{1z})$
$\mathrm{Im}(E_{1z})$
$\mathrm{Re}(B_{1y})$
$\mathrm{Im}(B_{1y})$
r/λ_a
(a)
(b)

Fig. 3

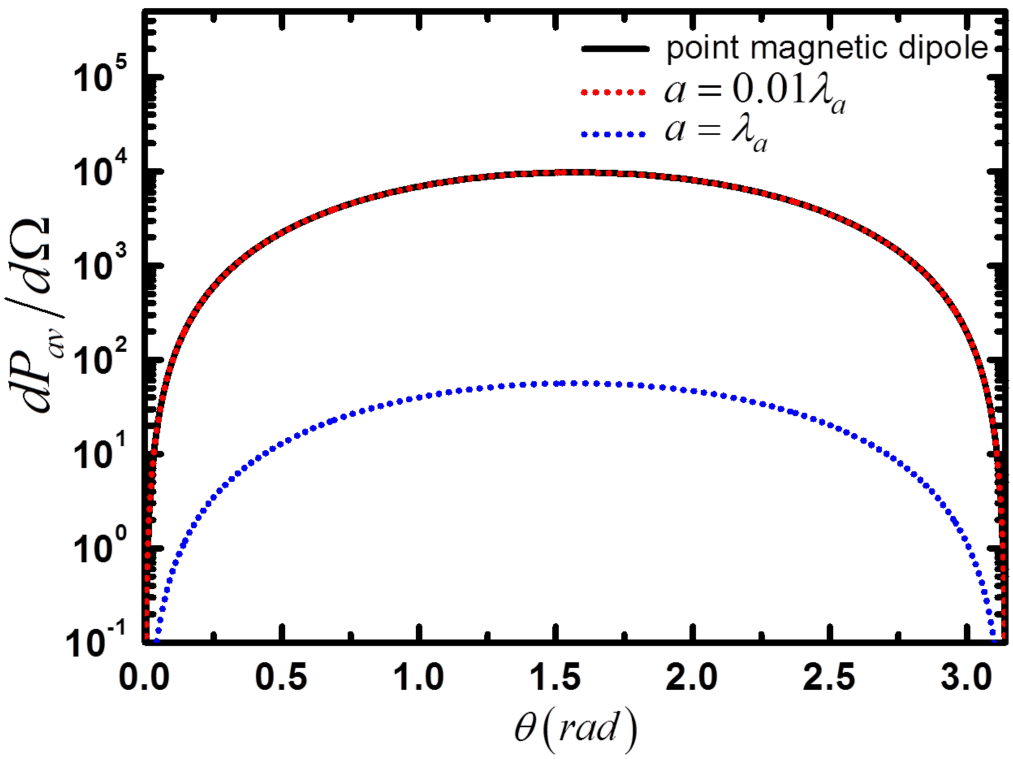
point magnetic dipole
$a = 0.01\lambda_a$
$a = \lambda_a$
10^5
10^4
10^3
10^2
10^1
10^0
10^{-1}
$dP_{av}/d\Omega$
0.0
0.5
1.0
1.5
2.0
2.5
3.0
$\theta(rad)$

Fig. 4